



2 Modeling the effects of throughfall reduction on soil 3 water content in a Brazilian Oxisol under a moist 4 tropical forest

5 Elizabeth L. Belk,^{1,2} Daniel Markewitz,¹ Todd C. Rasmussen,¹
6 Eduardo J. Maklouf Carvalho,³ Daniel C. Nepstad,⁴ and Eric A. Davidson⁴

7 Received 11 September 2006; revised 19 April 2007; accepted 24 May 2007; published XX Month 2007.

8 [1] Access to water reserves in deep soil during drought periods determines whether or
9 not the tropical moist forests of Amazonia will be buffered from the deleterious effects
10 of water deficits. Changing climatic conditions are predicted to increase periods of drought
11 in Amazonian forests and may lead to increased tree mortality, changes in forest
12 composition, or greater susceptibility to fire. A throughfall reduction experiment has been
13 established in the Tapajós National Forest of east-central Amazonia (Brazil) to test the
14 potential effects of severe water stress during prolonged droughts. Using time domain
15 reflectometry observations of water contents from this experiment, we have developed a
16 dynamic, one-dimensional, vertical flow model to enhance our understanding of
17 hydrologic processes within these tall-stature forests on well-drained, upland, deep
18 Oxisols and to simulate changes in the distribution of soil water. Simulations using
19 960 days of data accurately captured mild soil water depletion near the surface after
20 the first treatment year and decreasing soil moisture at depth during the second treatment
21 year. The model is sensitive to the water retention and unsaturated flow equation
22 parameters, specifically the van Genuchten parameters θ_s , θ_r , and n , but less sensitive to K_s
23 and α . The low root-mean-square error between observed and predicted volumetric soil
24 water content suggests that this vertical flow model captures the most important
25 hydrologic processes in the upper landscape position of this study site. The model
26 indicates that present rates of evapotranspiration within the exclusion plot have been
27 sustained at the expense of soil water storage.

29 **Citation:** Belk, E. L., D. Markewitz, T. C. Rasmussen, E. J. M. Carvalho, D. C. Nepstad, and E. A. Davidson (2007), Modeling the
30 effects of throughfall reduction on soil water content in a Brazilian Oxisol under a moist tropical forest, *Water Resour. Res.*, 43,
31 XXXXXX, doi:10.1029/2006WR005493.

33 1. Introduction

34 [2] Tropical rain forests have a disproportionate impor-
35 tance in the global exchange of carbon, water, and energy
36 between the biosphere and atmosphere [Schlesinger, 1997].
37 While the function of the Amazon river basin in the global
38 water cycle is well recognized, we are only beginning to
39 understand the interaction of factors affecting the below-
40 ground partitioning and availability of water and nutrients to
41 the vegetation in its forest ecosystems. These processes are
42 important for interpreting how humid tropical forests manage
43 to maintain evergreen canopies during the annual dry season
44 and for predicting how these forests might respond to
45 prolonged periods of drought, such as those that result from
46 El Niño–Southern Oscillation (ENSO) events [Nepstad et al.,
47 2004; Oliveira et al., 2005].

[3] To study the response of a humid Amazonian forest to
severe drought, a partial throughfall exclusion study was
initiated in 1998 in the Tapajós National Forest, east-central
Amazonia, near Santarém, Brazil [Nepstad et al., 2002].
This experiment compares two 1-ha plots, one of which
receives natural rainfall, while the other has plastic panels
installed in the forest understory during the rainy season.
These panels capture approximately 60 percent of incoming
throughfall, channelling the water to a system of gutters and
diverting it from the soil. Both the control and exclusion
plots are surrounded by a 1.0–1.7 m deep trench, which
reduces the ability of trees within the plots to access water
from outside the plots [Sternberg et al., 2002].

[4] A variety of processes are being monitored, including:
tree growth and mortality, sap flow, litterfall, leaf area
index, forest floor decomposition, soil respiration, trace
gas emissions, forest floor flammability, and the amounts
and chemistry of precipitation, throughfall, litter leachate,
and soil solutions. Soil moisture content is also measured by
time domain reflectometry using soil shafts that allow
access to 12 m depth in both the exclusion and control
plots. Soil moisture measurements alone, however, do not
describe the magnitudes and rates of water fluxes because
two layers may contain the same water volume within a

¹Warnell School of Forestry and Natural Resources, University of Georgia, Athens, Georgia, USA.

²Now at U.S. Environmental Protection Agency, Atlanta, Georgia, USA.

³Embrapa Amazônia Oriental, Belém, Brazil.

⁴Woods Hole Research Center, Woods Hole, Massachusetts, USA.

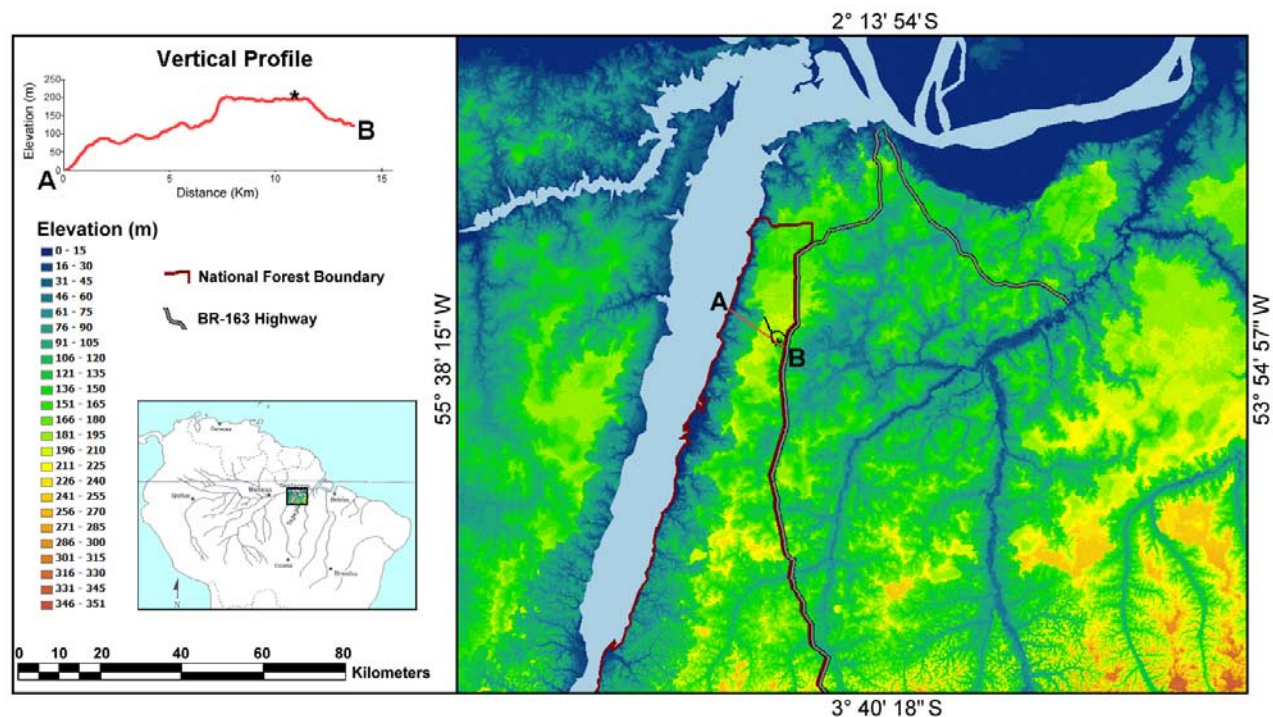


Figure 1. Site location for the throughfall exclusion experiment in the Tapajós National Forest, Brazil. Star in the top left plot indicates the research site location.

72 given soil volume, but have different rates of fluid movement
 73 through them. This means that model estimations of
 74 water fluxes are required in order to fully quantify the
 75 hydrologic system.

76 [5] The objective of this component of the throughfall
 77 reduction study is to develop an understanding of the
 78 physical processes driving the observed soil water dynamics
 79 at the site. We will make use of a vertically integrated
 80 version of the Richard's mass balance equation to evaluate
 81 the sensitivity of various parameters and to compare the
 82 hydrologic mass balance of the control and dry-down plots.
 83 Hydrologic flux estimates from this model might also be
 84 utilized in the future to estimate the advective movement of
 85 dissolved chemical components through the soil.

86 [6] Knowledge of the changes in below-ground storage
 87 and partitioning of water enhances our ability to explain
 88 other responses of the forest to drought conditions. By
 89 quantifying how the ecological functions of tropical forests
 90 change during prolonged drought, we hope to better under-
 91 stand the changes that may occur during the annual dry
 92 season in functions such as rooting depth or leaf shedding
 93 and better predict the ability of these forests to tolerate
 94 reductions in precipitation associated with land use conver-
 95 sion as well as long-term climate changes.

96 2. Tapajós Research Site

97 [7] The forest being modeled is located in a protected
 98 area of Floresta Nacional Tapajós, a Brazilian national forest
 99 located in east-central Amazonia, south of the city of
 100 Santarém do Pará (2.89°S, 54.95°W), shown in Figure 1.
 101 The site is located approximately 150 m above and 13 km
 102 east of the Tapajós River [Nepstad *et al.*, 2002]. The study
 103 plots are situated on a relatively level, upper landscape

plateau position where the soils are predominantly Haplus- 104
 tox (Latasolos vermelhos) dominated by kaolinite clays, and 105
 support a terra firme forest, which is a dense, humid, 106
 evergreen forest that does not flood annually. The forest at 107
 the field site has a continuous canopy that is approximately 108
 30 m tall. 109

[8] The throughfall reduction experiment was initiated in 110
 1998. After a 1-year pretreatment period, plastic panels 111
 were installed at the beginning of the 2000 rainy season 112
 that extends from January to May. Panels are removed 113
 during the dry season and reinstalled prior to the rainy 114
 season of the following year. 115

117 2.1. Soil Moisture

[9] Volumetric water contents ($m_w^3 m_s^{-3}$) were measured 118
 using time domain reflectometry (TDR) [Topp *et al.*, 1980] 119
 sensors installed to 11-m depth in six soil shafts (two plots; 120
 three shafts per plot; yielding six sensors per depth for both 121
 plots). Each soil shaft measures 1 m by 2 m in width, and 122
 extends to a depth of 12 m. Access is obtained using a 123
 system of wooden beams and supports. 124

[10] TDR sensors consist of three, parallel, 24-cm stain- 125
 less steel rods [Zegelin *et al.*, 1989] and were measured with 126
 a cable tester (Textronix 1502C, Beaverton, Oregon). Two 127
 TDR sensors were installed horizontally in opposing walls 128
 at 1-m increments in each soil shaft. Each of the six shafts 129
 also has two probes installed vertically from 0 to 0.3 m, and 130
 two probes installed horizontally at 0.5 m. Because the 131
 shafts were left open to maintain access for root and nutrient 132
 studies, sensors were installed into undisturbed soil 1.5 m 133
 from the shaft walls. Auger holes were back filled with 134
 native soil. This installation method was based on previous 135
 work in Oxisols in Paragominas, Pará [Davidson and 136
 Trumbore, 1995]. 137

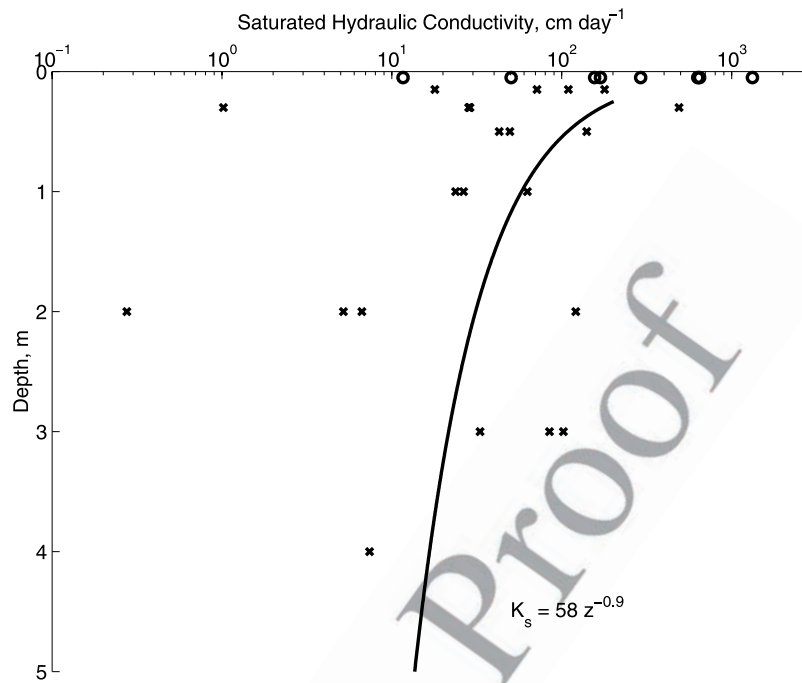


Figure 2. Surface (circles) and subsurface (crosses) measurements of saturated hydraulic conductivity, K_s , in the Tapajós National Forest, Brazil. The K_s values between 0 and 4 m were measured with a Guelph permeameter. Extrapolation to greater depths uses a power function fit.

138 [11] Waveforms from the TDR sensors were collected
 139 approximately once per month. Water contents were esti-
 140 mated following the methods of *Topp et al.* [1980]. The
 141 Topp equation has been validated for mineral soils in both
 142 surface and deep Oxisols in the Amazon by *Jipp et al.*
 143 [1998]. The Belterra clay soil used in the validation study
 144 are the same as the soils studied here, and have similar
 145 physical characteristics.

147 2.2. Saturated Hydraulic Conductivity

148 [12] Saturated hydraulic conductivity (K_s) was quantified
 149 using a Guelph permeameter [it *SoilMoisture Equipment*
 150 *Corporation*, 1986]. Seven surface measurements were
 151 made in random locations around the plots using a pressure
 152 infiltrometer attachment. Figure 2 presents K_s results from
 153 the surface to 4 m. Below-ground observations were
 154 obtained by augering 6-cm-diameter vertical holes. Three
 155 sets of measurements were completed at each of three sites
 156 in the study area. The holes were gently brushed before
 157 measurements to remove any smearing of the clays that may
 158 have occurred during augering.

159 [13] K_s results from the surface and at 30 cm are pre-
 160 sented in Figure 2. Note the large variation in observations,
 161 which is consistent with other sites [*Rasmussen et al.*,
 162 1993]. Data were arithmetically averaged at each depth
 163 and assigned to the closest layer midpoint. Because our
 164 model extends to greater depths, estimates of deeper values
 165 are required. We are not aware of any studies that have
 166 measured K_s to 11 m depth. It is likely, however, that K_s
 167 decreases with depth, because K_s is highly affected by
 168 macroporosity and these deep soils become less structured
 169 with depth in this region. This hypothesis is supported by
 170 the resulting fit of a power function to the observed data
 171 (also shown on Figure 2), which indicates a decrease with

depth. Point estimates of K_s were extrapolated using this
 power function for soil layers between 4 and 11 m.

172 2.3. Rainfall and Throughfall

173 [14] Rainfall was estimated from three, prism-shaped
 174 gauges located in and near the study site. One gauge was
 175 installed within each plot on the top of a 28-m tower within
 176 a small canopy opening. One additional gauge was located
 177 at ground level in an opening approximately 400 m from the
 178 plots. Rainfall was monitored daily, except over the week-
 179 end; Monday readings include rain that fell over the
 180 weekend; Monday readings include rain that fell over the
 181 weekend.

182 [15] Throughfall samples were collected in 0.16-m-diam-
 183 eter funnels that lead to plastic collection bottles. Each plot
 184 has ten throughfall collectors under the canopy. Bottles were
 185 at ground level during the pretreatment year. In the follow-
 186 ing years all bottles were raised approximately 2 m above
 187 ground level so that exclusion panels did not interfere with
 188 throughfall collection. Sample volumes were measured
 189 every two weeks. The ten collectors in each plot were
 190 randomly reassigned a location within the sampling grid
 191 for that plot after each sampling.

192 2.4. Fine-Root Biomass

193 [16] Fine root biomass data (kg m^{-2}) were estimated
 194 from 24 borings divided into eight depths in each plot
 195 (384 samples). Each sample was washed and sorted into live
 196 and dead fractions, and then sorted into two size classes
 197 (<1 mm and 1–2 mm). The depths at which samples were
 198 collected were: 0, 0.5, 1, 2, 3, 4, 5, and 6 m. The fraction of
 199 the total fine (live) root biomass (0–2 mm) in each layer
 200 was used to estimate a rooting factor, $R(z)$, for each modeled
 201 soil layer. The root biomass was considered to be 10 percent
 202 of the total fine root biomass in each layer.

205 less than the horizon above for estimating root factors below
206 6 m.

208 2.5. Soil Moisture Parameters

209 [17] Soil water retention data were generated by the
210 EMBRAPA-CPATU laboratory in Belém, Pará, Brazil. A
211 standard pressure plate method was used whereby intact soil
212 cores (n = four per depth) were saturated and the water
213 extracted by the application of a steady, constant pressure
214 [Klute and Dirksen, 1986].

215 [18] These data were fit to van Genuchten soil moisture
216 characteristic (SMC) functions using nonlinear regression
217 [Wraith et al., 1993]. The starting values for the nonlinear
218 regressions were the average van Genuchten parameters (α ,
219 θ_s , θ_r , and n) reported by Hodnett and Tomasella [2002] for
220 tropical clay soils.

222 2.6. PET and Other Meteorological Data

223 [19] Potential evapotranspiration (PET) was calculated
224 using the Thornthwaite method [Thornthwaite and Mather,
225 1957]. On-site temperature data were available for estima-
226 tion with this method and thus avoided additional parame-
227 terization (e.g., stomatal conductance) that would have been
228 required with methods such as Penman-Monteith [Monteith,
229 1965]. An eddy flux tower was established in close prox-
230 imity to the experimental site in 2000 but direct estimates of
231 AET are only available after 2002 [Hutyra et al., 2005].
232 Data from this eddy flux tower, however, did demonstrate a
233 strong correlation between AET and PET estimated with the
234 Thornthwaite method [Hutyra et al., 2005]. For the current
235 model, temperature inputs utilized were monthly averages
236 of daily daytime air temperatures collected at the canopy
237 level of the control plot with recording Hobo data loggers
238 (Onset Computer Corp., Bourne, Massachusetts). An addi-
239 tional correction was applied to this estimate to adjust for
240 the tendency of the Thornthwaite model to overestimate
241 PET when average air temperature is greater than 26.5°C
242 [de Amorim et al., 1999]. This correction is based on an
243 empirical fit and has the following form:

$$244 \quad PET \geq 26 = PET^* \left(1 - e^{-0.28*(t-31.1)} \right) \quad (1)$$

245 where t is the mean monthly temperature. After all
246 corrections, the monthly estimates of PET were divided
247 into equal daily values to be consistent with the time step of
248 the model.

250 3. Soil Water Model

251 3.1. Model Structure

252 [20] The model was designed to simulate daily changes in
253 the distribution of soil water. Vertical water movement
254 through 13 soil layers is driven by the difference in total
255 soil hydraulic head, which integrates the effect of matric and
256 gravitational forces. Plant uptake of water to the forest
257 vegetation is included. Simulations were performed for
258 the control plot with no reduction in water inputs and for
259 the treatment plot using throughfall exclusion during the
260 rainy season.

261 [21] The model used a daily time step, but changes in
262 VWC were integrated using the Euler method on an hourly
263 basis. The Euler method estimates changes in stocks using

Table 1. Model Inputs^a

Input	Description	Units	
<i>Soil Water Model Parameters</i>			
Rainfall	daily rainfall rate	mm d ⁻¹	t1.3
PET	daily potential evapotranspiration	mm d ⁻¹	t1.4
Throughfall	rainfall entering soil surface	fraction	t1.5
$\Delta z(z)$	distance between layers	m	t1.6
H(z)	total hydraulic head	m	t1.7
D _w (z)	water depth in soil layer	m	t1.8
K _s (z)	saturated hydraulic conductivity	m s ⁻¹	t1.9
R(z)	root length or biomass present	fraction	t1.10
<i>van Genuchten Parameters</i>			
$\theta_s(z)$	saturated water content	m _w ³ m _v ⁻³	t1.11
$\theta_r(z)$	residual water content	m _w ³ m _v ⁻³	t1.12
$\alpha(z)$	water retention	m ⁻¹	t1.13
n(z)	water retention	-	t1.14

^aParameters with (z) are input for each layer of soil.

the computed flow values. Given larger time steps (i.e., 264
1 day) this algorithm is preferred. Calibration was per- 265
formed using soil volumetric water content measured in 266
the control plot on an approximately monthly interval 267
during the first 960 days of the experiment. When the 268
throughfall exclusion treatment switch is selected the model 269
predicts soil volumetric water content for the same time 270
period as the forest undergoes partial throughfall exclusion 271
without any additional calibration of the model. 272

[22] The temporal (Δt) and vertical (Δz) discretization of 273
this model were chosen to be consistent with the scale of the 274
data available for validation (i.e., monthly TDR data for soil 275
layers of 50 to 100 cm). Finer-scale discretization (i.e., $\Delta t \leq$ 276
1 day and $\Delta z \leq 5$ cm), however, is often preferred for 277
applications of the Richard's equation particularly with 278
regard to surface soil layers [Lee and Abriola, 1999]. To 279
test the affect of these temporal and vertical discretizations 280
HYDRUS 1D was utilized [Šimůnek et al., 2005]. HYD- 281
RUS 1D was parameterized utilizing the same data de- 282
scribed below although the 13 soil layers over the 11.5 m 283
profile were discretized into 5 cm increments for model 284
solution. 285

287 3.2. Model Inputs

[23] Table 1 contains a list of the inputs required by the 288
model. The depths separating each of the 13 soil layers are: 289
0, 0.4, 0.75, 1.5, 2.5, 3.5, 4.5, 5.5, 6.5, 7.5, 8.5, 9.5, 10.5, 290
and 11.5 m. These increments were chosen so that the TDR 291
measurements are near the midpoints of each layer. Other 292
site-specific information, such as air temperature for PET 293
estimates, is implicitly incorporated within the model. 294

296 3.3. Forest Water Inputs

[24] Rainfall enters the forest system and is partitioned 297
between throughfall and canopy interception (Figure 3). 298
Throughfall was empirically determined at the site to be 299
88 percent of incoming rainfall; the balance, 12 percent, is 300
intercepted by the canopy. This empirical relationship did 301
not vary by season and data were not available to test a 302
relationship with rainfall intensity. Furthermore, coverage of 303
the canopy, which is usually around 95 percent, did not 304
change in either plot during the simulation period [Nepstad et 305
al., 2002]. When the treatment plot is simulated, 60 percent 306
of the throughfall input is diverted from the soil when 307
the panels are in place. This throughfall exclusion estimate 308

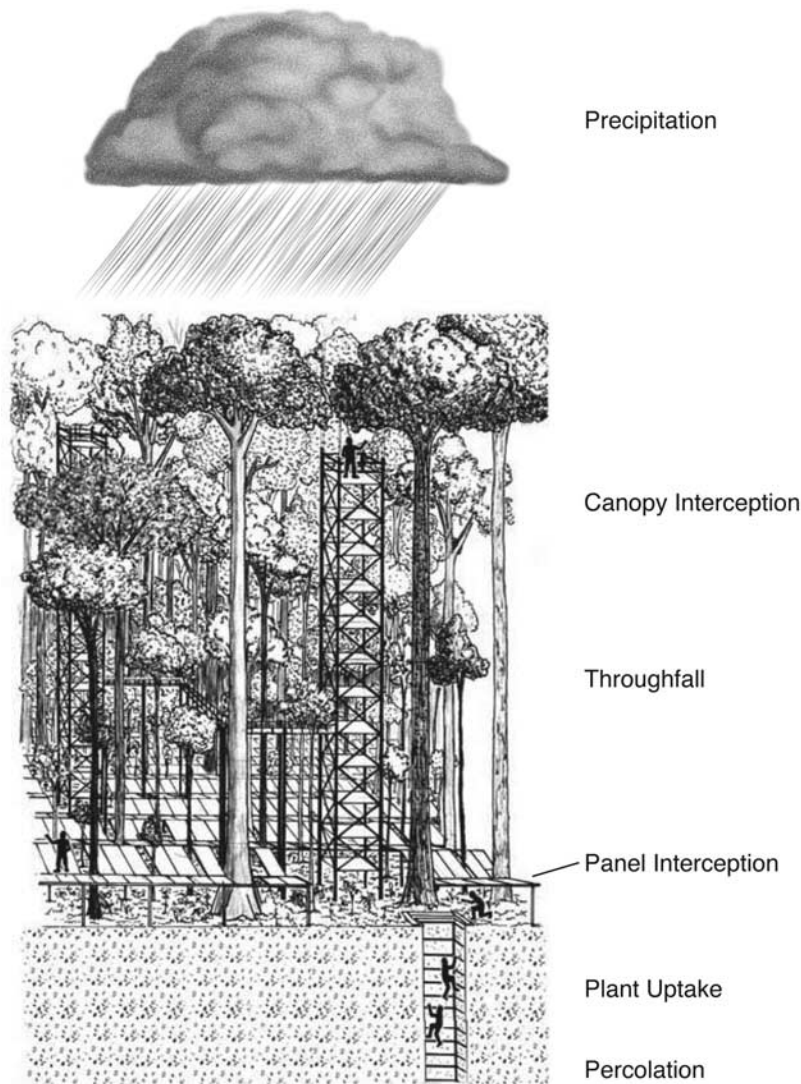


Figure 3. Idealized model structure for water cycling in a deep Oxisol. Precipitation, panel interception, and soil water contents were measured. Empirical functions were used for canopy interception and plant root uptake.

309 is based on measurements of water volumes collected in the
310 gutters transporting water off the plot [Nepstad *et al.*, 2002].

312 3.4. Soil Water Movement

313 [25] Throughfall reaching the soil surface is allowed to
314 infiltrate directly into the uppermost soil layer because the
315 litter layer on the site is thin (approximately 2–4 cm) and
316 the measured surface infiltration rates were high ($>30 \times$
317 10^{-6} m s^{-1}). All thirteen layers hold a depth of water
318 (D_w , m) equivalent to the soil moisture within that incre-
319 ment of soil. The water depth in each layer was initialized
320 using soil water content data from May 17, 1999, the first
321 day of simulation. The water content of each layer ($\theta(z) =$
322 $D_w(z)/\Delta z$; $\text{m}^3 \text{ m}^{-3}$) is determined using the depth of water
323 (D_w ; m) and the soil thickness (Δz ; m).

324 [26] Water flux between soil layers is determined using
325 Darcy's law for one-dimensional (vertical), unsaturated flow
326 [Muller, 1999]:

$$q_z = K(\theta) \frac{\Delta H}{\Delta z} \quad (2)$$

where q_z is the vertical water flux (m s^{-1}), $K(\theta)$ is the
328 unsaturated hydraulic conductivity (m s^{-1}), ΔH is the
329 difference in total hydraulic head between two adjoining
330 layers (m) and Δz is the downward directed, vertical
331 distance between the midpoints of the layers (m). 332

[27] The total hydraulic head of the soil water, $H(z) = h_m +$
333 h_z , in a given layer is the sum of the matric (h_m) and
334 gravitational (h_z) heads. The matric head of the soil water is
335 determined by the van Genuchten equation relating water
336 content to matric head [van Genuchten, 1980]: 337

$$h_m = \frac{1}{\alpha} \left[\Theta^{-1/m} - 1 \right]^{1/n} \quad (3)$$

where $\Theta = (\theta - \theta_r)/(\theta_s - \theta_r)$ is the relative saturation of the
339 soil ($\text{m}^3 \text{ m}^{-3}$), and where θ_s is the saturated water content, 340
 θ_r is the residual water content, and α (m^{-1}), n , and $m = 1 -$
341 $1/n$ are fitting parameters. 342

[28] The soil surface serves as the datum where gravita-
343 tional head is zero. Unsaturated hydraulic conductivity, 344

345 $K(\theta)$, is calculated from saturated hydraulic conductivity,
 346 K_s , values according to the equation of *Mualem* [1976]:

$$K(\theta) = K_s \Theta^{1/2} \left[1 - \left[1 - \Theta^{n/(n-1)} \right]^m \right]^2 \quad (4)$$

349 [29] Changes in soil water storage are modeled using the
 350 Richard's (mass balance) equation that accounts for inflows
 351 and outflows in each layer:

$$\frac{\partial q_z(z)}{\partial z} \pm U(z) = \frac{\partial \theta(z)}{\partial t} \quad (5)$$

353 where $U(z)$ are internal sources or sinks within each layer.
 354 Root uptake (described below) is the only mechanism for
 355 internal water loss within each layer in our model.

357 3.5. Deep Drainage

358 [30] Deep drainage out of the lowest layer ($\text{m}^3 \text{m}^{-2} \text{s}^{-1}$)
 359 is calculated using Darcy's law and the assumption that
 360 saturated conditions persist at great depth, which is consistent
 361 with an observed water table depth of 100 m [*Nepstad*
 362 *et al.*, 2002]. Because the matric head is zero at the water
 363 table, i.e., $h_m = 0$, the total head must equal the gravitational
 364 head ($H = h_z = z$). This lower boundary condition may have
 365 some effect on the simulated drainage rate from the lowest
 366 layer, but has less of an influence on the water content of the
 367 profile overall.

369 3.6. Soil Evaporation and Plant Uptake

370 [31] The model assumes that there is no evaporation from
 371 the soil surface because only about 1 percent of solar
 372 radiation penetrates the forest canopy [*Nepstad et al.*,
 373 2002]. Other researchers have reported that direct evaporation
 374 from the soil surface is negligible in Amazonian forests
 375 [*Jordan and Heuvelop*, 1981]. Water required for transpiration
 376 by vegetation is removed from each soil layer before
 377 downward percolation is allowed. It is assumed that when a
 378 vapor pressure deficit exists between the forest and surrounding
 379 atmosphere, water evaporates from vegetative
 380 surfaces more readily than it can be transpired through leaf
 381 stomata [*Ubarana*, 1996].

382 [32] Intercepted water in the canopy is first used to satisfy
 383 evapotranspirational demand, which is determined by the
 384 PET. Intercepted water is temporarily stored within the
 385 canopy and allowed to evaporate directly from it at a rate
 386 limited by the PET. If more water is intercepted than can be
 387 potentially evapotranspired, then no water is taken from the
 388 soil during that time step. When the PET is greater than the
 389 amount of water stored within the canopy, then water is
 390 removed from the soil in an amount equal to the difference.
 391 The fraction of this total uptake extracted from a given layer
 392 is

$$U(z) = U_{\max} R(z) URF(z) \quad (6)$$

394 where U_{\max} is the maximum amount of water extracted
 395 from the soil (m), $R(z)$ is the proportion of fine root biomass
 396 in a given layer, and $URF(z)$ is an uptake reduction factor
 397 that restricts plant uptake on the basis of the matric head.
 398 URF does not vary with PET, and uptake near saturation is
 399 not restricted [*Feddes et al.*, 1978, 2001].

[33] Thornthwaite calculations were performed independent of, and prior to, model simulation and were then provided as a daily input for simulation. Because water content calculations were reported on an approximately monthly basis, the failure to account for intradaily PET variation is not expected to substantially affect model calculations.

377 3.7. Model Sensitivity and Performance

[34] Sensitivity analysis were performed on the saturated hydraulic conductivity (K_s) and VG parameters (i.e., α , θ_s , θ_{rs} , m , and n). The parameter of interest was assigned at least five other values while the remaining parameters were left unchanged. The sensitivity of the model to these changes was quantified by evaluating their effect on the average depth of water stored in that layer, layers above or below, and/or the average depth of water in the entire profile. Model performance was evaluated using the mean difference, root-mean-square error (RMSE), relative root-mean-square-error (RRMSE), and the coefficient of determination (R^2) between measured and predicted volumetric water content.

4. Results and Discussion

4.1. Model Calibration

[35] We endeavored to use only input variables or constants that were determined by measurements made at the site for the initial parameterization of the model (Table 2, but see below). It became apparent during parameterization, however, that the model was unstable when there were large changes in the VG parameters between soil layers. These large differences between adjacent layers may allow one or more layers to wet or dry beyond reasonable ranges. The VG parameters fit to laboratory-generated water retention data for the site demonstrated this characteristic, largely in the upper layers, and thus the model was unstable.

[36] Inconsistencies in physical soil water characteristics between laboratory and field data are not uncommon [*Rasmussen et al.*, 1993]. One reason for the poor correspondence is the alteration of soil structure during sample collection, resulting in an increase in overall macroporosity. Another reason is an artifact of laboratory testing, in that soils are normally tested by drying the samples, yet soil moisture changes under field conditions include both wetting and drying conditions (i.e., hysteresis effects). Spatial variability of soil properties is another possible explanation. Finally, it is possible that the laboratory data is correct but that the numerical method utilized in the model was insufficient to adequately represent the true variation.

[37] VG parameters for each soil layer were calibrated iteratively using data from the control plot until RMSE between the measured and predicted volumetric water content for all depths over all dates was minimized (Figure 4). The resulting RMSE is 1.88 percent water content, which is a RRMSE of 5.1 percent.

[38] The soil moisture characteristic (SMC) curves that result from the optimized VG parameters are displaced below the laboratory data (Figure 5). In other words, calibrated water contents are drier than the laboratory values when compared at the same matric suction. In all cases, laboratory data have the lowest average range of water content between the saturated, θ_s , and residual, θ_{rs} , water content ($0.216 \text{ m}_w^3 \text{ m}_s^{-3}$). The laboratory SMC curve has the

t2.1 **Table 2.** Parameter Values and Initial Values for Stocks Input for Each Model Layer^a

t2.3	Layer	Depth, m	Initial D_w		$K_s, \mu\text{m s}^{-1}$	van Genuchten Parameters				
			Control, m	Treatment, m		$\theta_s, \text{m}^3 \text{m}^{-3}$	$\theta_r, \text{m}^3 \text{m}^{-3}$	α, m^{-1}	n	R
t2.4	1	0–0.4	0.155	0.125	31.69	0.44	0.24	0.040	1.2	0.688
t2.5	2	0.4–0.75	0.106	0.109	8.98	0.41	0.23	0.040	1.5	0.103
t2.6	3	0.75–1.5	0.247	0.225	4.35	0.40	0.21	0.040	1.5	0.050
t2.7	4	1.5–2.5	0.339	0.307	3.85	0.35	0.20	0.055	1.3	0.030
t2.8	5	2.5–3.5	0.370	0.325	8.50	0.46	0.22	0.050	1.5	0.022
t2.9	6	3.5–4.5	0.378	0.354	0.86	0.44	0.23	0.055	1.6	0.019
t2.10	7	4.5–5.5	0.415	0.374	1.64	0.47	0.23	0.050	1.4	0.019
t2.11	8	5.5–6.5	0.423	0.394	1.40	0.49	0.23	0.045	1.5	0.017
t2.12	9	6.5–7.5	0.433	0.399	1.23	0.49	0.22	0.045	1.4	0.015
t2.13	10	7.5–8.5	0.418	0.373	1.10	0.49	0.19	0.040	1.4	0.014
t2.14	11	8.5–9.5	0.414	0.386	0.98	0.47	0.21	0.045	1.4	0.012
t2.15	12	10.5–11.5	0.410	0.392	0.90	0.47	0.21	0.045	1.4	0.011
t2.16	13	11.5–12.5	0.406	0.413	0.82	0.46	0.20	0.040	1.4	0.010

^aInitial throughfall fraction is 0.88. Saturated hydraulic conductivity (K_s) was measured in the field for layers 1–6 but were extrapolated below layer 6 using the power function shown in Figure 1. Van Genuchten parameters ($\theta_s, \theta_r, \alpha$, and n) obtained from model calibration. Fraction of total, fine (0–2 mm) live root biomass (R) were measured in layers 1–8 but were extrapolated below layer 8 by assuming a reduction of 10 percent in each subsequent layer.

t2.17

462 highest water content, primarily due to a smaller average n
 463 value. This higher laboratory SMC curve for the surface soil
 464 yields a larger θ_r value than optimized values. In all cases,
 465 the optimized θ_s values are lower than the porosities
 466 measured in the laboratory. Values for α are also moderately
 467 higher, which reflects the presence of pores that empty with
 468 small changes in matric head.

469 [39] For comparison, Figure 5 also presents an average
 470 SMC curve for tropical soils with clay textures, as well as an
 471 average SMC curve for Ferralsols [Hodnett and Tomasella,
 472 2002]. Both soils contain kaolinite clays which do not swell
 473 and tend to have higher α values because they drain from
 474 saturation quickly [Hodnett and Tomasella, 2002]. Note that
 475 the optimized SMC curve resembles the average for tropical
 476 Ferralsols. The soils at the study site being modeled are
 477 classified as Latosols in the Brazilian taxonomy, which is
 478 similar to the FAO definition of a Ferralsol [Richter and
 479 Babbar, 1991]. The most notable difference between the
 480 parameters is that the average range of water content ($\theta_s - \theta_r$)

for the optimized parameters is much lower, $0.234 \text{ m}^3 \text{m}^{-3}$
 compared to an average of $0.322 \text{ m}^3 \text{m}^{-3}$ for the Ferralsols.

[40] Regardless of these discrepancies, using the difference
 between the water contents at 30 and 1500 kPa to represent the
 maximum plant-available water (PAW), it is clear that all SMC
 curves contain 6.2–6.9 percent PAW.

[41] For the calibrated simulation, the top two layers have
 poorer fits than the others, with RRMSEs of 9.8 percent or
 greater (Figure 6). Except for the third layer, which has an
 RRMSE of 5.4 percent, the errors in the other horizons are
 all below 4.6 percent. The poorer fit in the top horizons, did
 not result simply from the coarse vertical discretization of
 the model as evidenced by comparison to the 5-cm discretization
 of the HYDRUS 1D model (Figure 7). Simulations from both
 models demonstrate similar seasonal patterns and

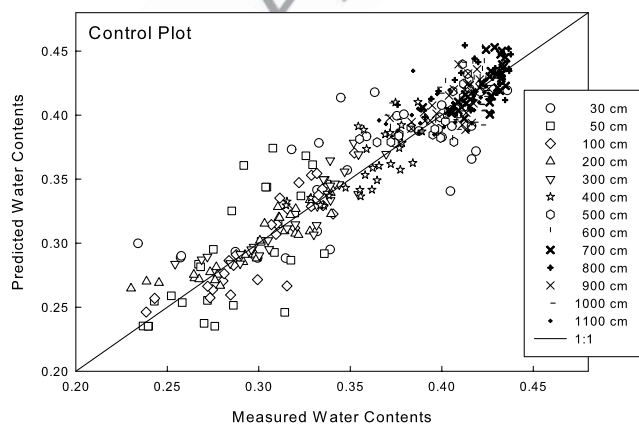


Figure 4. Scatterplot of measured and predicted volumetric water contents (θ) in the control plot, Tapajós National Forest, Brazil. The comparison is for 13 depths and 29 dates between May 1999 and December 2001 on which water content (θ) was measured at the field site.

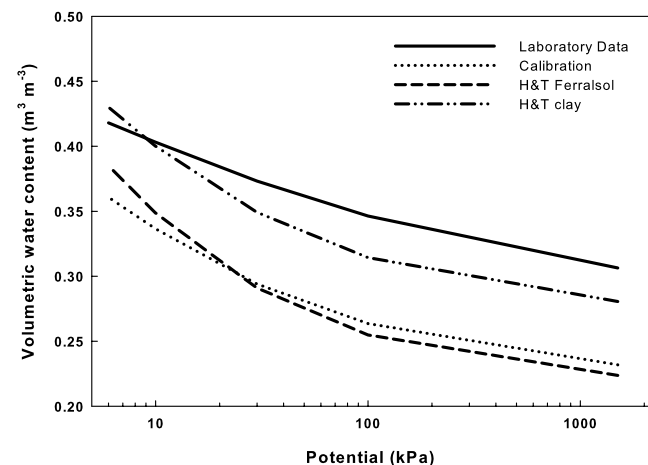


Figure 5. Soil moisture characteristic curves described by the van Genuchten parameters fit to laboratory pressure plate data and by the parameters resulting from model calibration. For comparison, the curves described by the average parameters for tropical soils with clay textures and for tropical soils in the Ferralsol soil group as reported by Hodnett and Tomasella [2002] are shown. All curves are for upper surface soils (<10 cm).

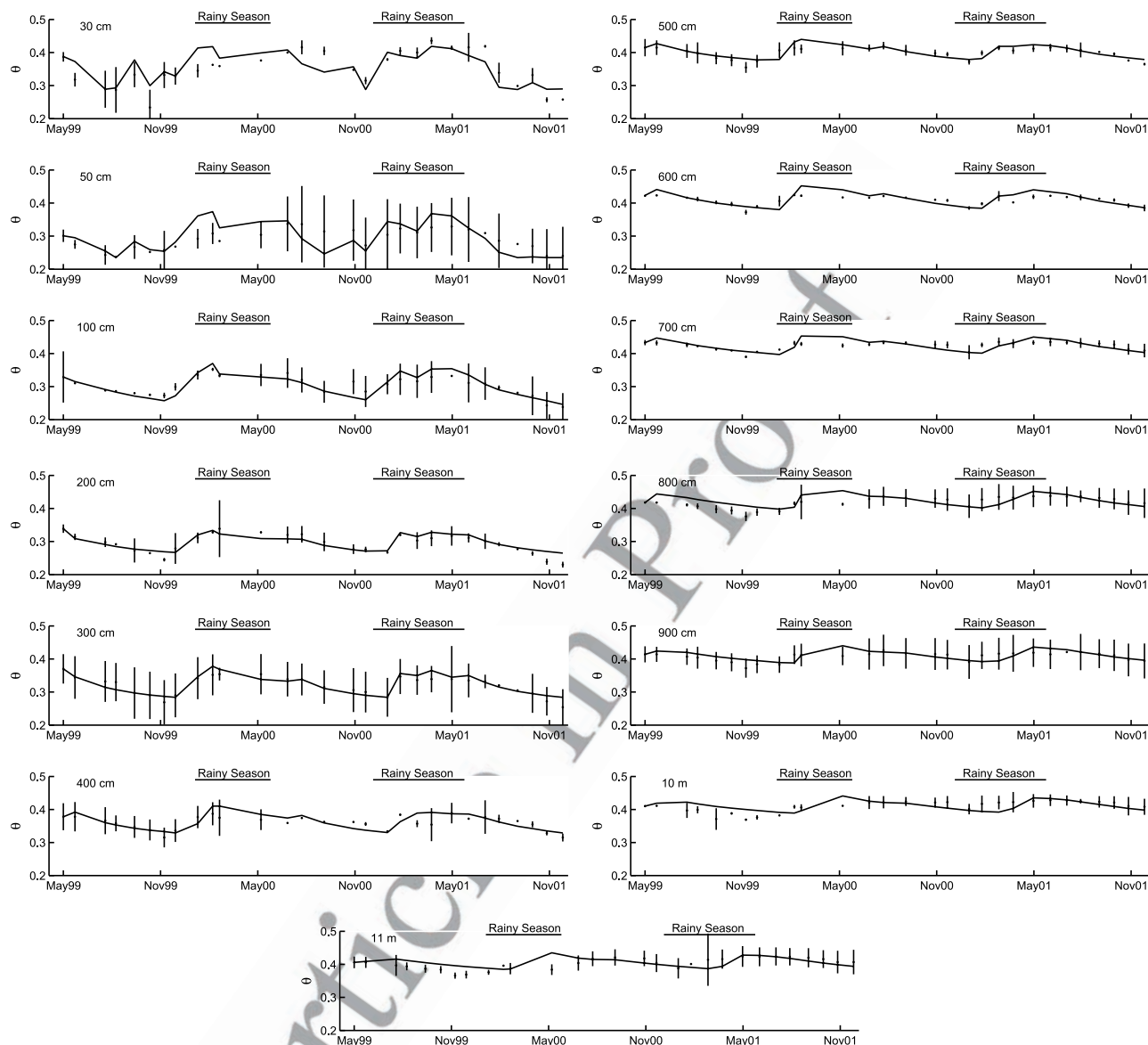


Figure 6. Monthly measured (dots) versus predicted (lines) volumetric water contents (θ) in the control plot, Tapajós National Forest, Brazil. Measured θ are averages of six TDR sensors per depth. Also shown are vertical bars representing measurement standard deviations, where available.

496 both tend to underestimate the wettest measurements while
 497 over estimating the driest measurements. Surface soils
 498 clearly undergo a great deal of variation in VWC and both
 499 model discretizations struggle to capture this variance where
 500 the soil moisture conditions are more dynamic. Limited
 501 discretization of inputs to the model (e.g., daily rainfall or
 502 daily average PET) may also limit the ability to capture
 503 surface soil dynamics. In the lower depths where VWC is
 504 more static both models perform well.

505 [42] The calibrated STELLA model does succeed in
 506 capturing important seasonal trends and shows the expected
 507 delay in recharge and depletion responses with increasing
 508 depth. The timing of these delays, however, are about a
 509 month or two slow in the model predictions. This slower
 510 response is consistent with observations in other moist
 511 systems where empirical estimates of the hydraulic veloc-

ities are greater than estimates based on SMC functions, 512
 [Rasmussen *et al.*, 2000]. 513

4.2. Sensitivity Results 515

[43] We tested the sensitivity of the model to the input 516
 parameters using optimized parameters from the calibrated 517
 model (Table 2). Analyses show that the model is more 518
 sensitive to θ_s , θ_r , and n , but less sensitive to α and K_s 519
 (Figure 8). The sensitivity of the model to the VG parameters 520
 is not unexpected given that they are used in both the 521
 equation that determines matric heads and the equation for 522
 unsaturated hydraulic conductivities. For the parameters to 523
 which the model is most sensitive, however, the effect of a 524
 change in one layer is largely confined to that layer. For 525
 example, raising the θ_s in a layer from 0.40 to 0.60 (40– 526
 60 percent water content) increased the average soil moisture 527
 of that layer by 10.6–13.6 percent, but the average water 528

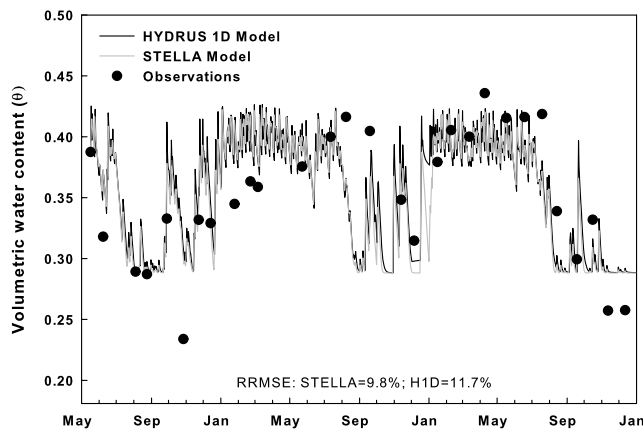


Figure 7. Comparison of monthly measured (dots) versus predicted (lines) volumetric water contents (θ) in the control plot using a coarse (one 40 cm layer in STELLA) or finer (eight 5 cm layers in HYDRUS 1D) model discretization. Measured θ are averages of six TDR sensors per depth in the Tapajós National Forest, Brazil.

529 content of the layer above or below generally decreased by
530 1 percent or less. The relative patterns in sensitivity remain
531 the same for the average water content of the entire profile,
532 but the increase is only 0.2–1.1 percent.

533 [44] Changing θ_r in a layer from 0.10 to 0.30 (10–
534 30 percent water content) increased the average soil mois-
535 ture of the layer by 3.8–8.5 percent. In contrast, a hundred-
536 fold increase in K_s resulted in only a 1–2 percent decrease
537 in the water content of a layer. The water content is
538 somewhat sensitive to K_s when the value is low because
539 K_s represents the maximum flow rate. Thus the soil water
540 content is affected whenever K_s is less than the water flux,
541 but increases in K_s above the water flux have little effect on
542 the water content.

543 [45] While the sensitivity of the model to individual
544 changes in VG parameters may be important, it is also
545 important to examine how the four parameters work together
546 to define the water retention and unsaturated flow rates. A full
547 factorial analysis of the interaction between θ_s , θ_r , and n for
548 the 1.5–2.5 m layer confirms that the model is also sensitive
549 to the difference between θ_s and θ_r . This difference is more
550 important than absolute values because it indicates the range
551 of water content expected in the soil (and the range for which
552 the van Genuchten and Mualem models are valid). The
553 difference between the average water content of the layer
554 when θ_s is high ($0.6 \text{ m}^3 \text{ m}^{-3}$) and θ_r is low ($0.1 \text{ m}^3 \text{ m}^{-3}$)
555 versus when θ_s is low ($0.4 \text{ m}^3 \text{ m}^{-3}$) and θ_r is high (0.3 m^3
556 m^{-3}) is about 2 percent, but when both parameters are low or
557 high the difference in water content was 19.5 percent.

559 4.3. Treatment Plot Predictions

560 [46] Using the VG parameter values calibrated within the
561 control plot, we simulated the soil water content in the
562 throughfall exclusion plot over the 960 days of available
563 data (Figure 9). The treatment plot shares similar throughfall
564 inputs as the control plot during the first eight months of the
565 simulation in May through December 1999. In 2000 and
566 2001, 895 and 817 mm of throughfall were excluded from
567 the treatment plot by the model, values slightly greater than

the 890 and 794 mm estimated empirically by *Nepstad et al.* 568
[2002]. 569

[47] Throughout this period of simulation the RMSE in
570 soil moisture is 3.1 percent water content. This is a RRMSE
571 of 9.2 percent. The mean difference is -0.65 ± 0.16 percent
572 water content. Any loss of soil contact with the TDR
573 sensors, due either to compaction during installation or to
574 later soil drying, could cause low soil moisture reading
575 [Baker and Lascano, 1989; Knight, 1992, 1994]. 576

[48] Overall, the treatment plot simulation model was
577 able to explain about 73 percent of the variability in the
578 volumetric water content data (Figure 10). The model
579 overpredicts lower TDR readings and slightly underpredicts
580 the wetter ones. The seasonality and timing of soil moisture
581 depletion and wetting of the treatment plot simulations
582 below 1 m also seem delayed by 1–3 months. Additionally,
583 from 6 to 11 m the model simulates a greater drawdown of
584 water than the TDR data indicate, especially during the
585 second posttreatment rainy season (Figure 9). 586

[49] The greater simulated drawdown in the deeper soil
587 layers could be due to incorrect assumptions regarding the
588 K_s or the root distribution or function in those layers. The K_s
589 values estimated by the power function may be too high,
590 which would drain these deeper layers too fast. The model
591 also lacks a mechanism to account for a change in the
592 distribution of fine roots. Fine root biomass down to 6 m at
593 this site was first estimated in August 2000. A second series
594 of root sampling was performed in July 2001, over 2 years
595 after the start of the experiment and about 1.5 years after the
596 treatment panels were first installed. Samples were collected
597 only between 0 to 2 m, corresponding to the depth where
598 most of the soil moisture depletion had occurred. The
599 results show no significant difference in root biomass
600 between the treatment and control plots [Nepstad et al.,
601 2002]. Deeper depths were not sampled, however, so it is
602 not known whether or how root biomass changed below
603 2 m. As the surface layers continue to dry, increased fine
604

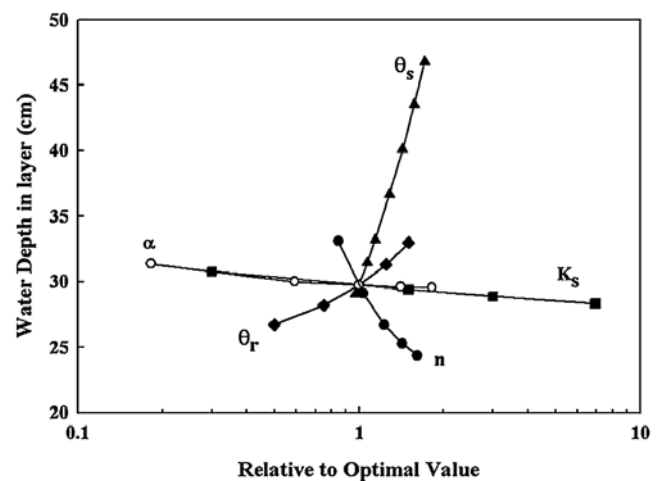


Figure 8. Sensitivity analysis of van Genuchten parameters (θ_s , θ_r , α , and n) and K_s for 1.5–2.5 m showing the effect of a change in the parameter values on the average depth of water in that layer over the 960-day simulation period. The change in parameter values is relative to the default values listed in Table 2.

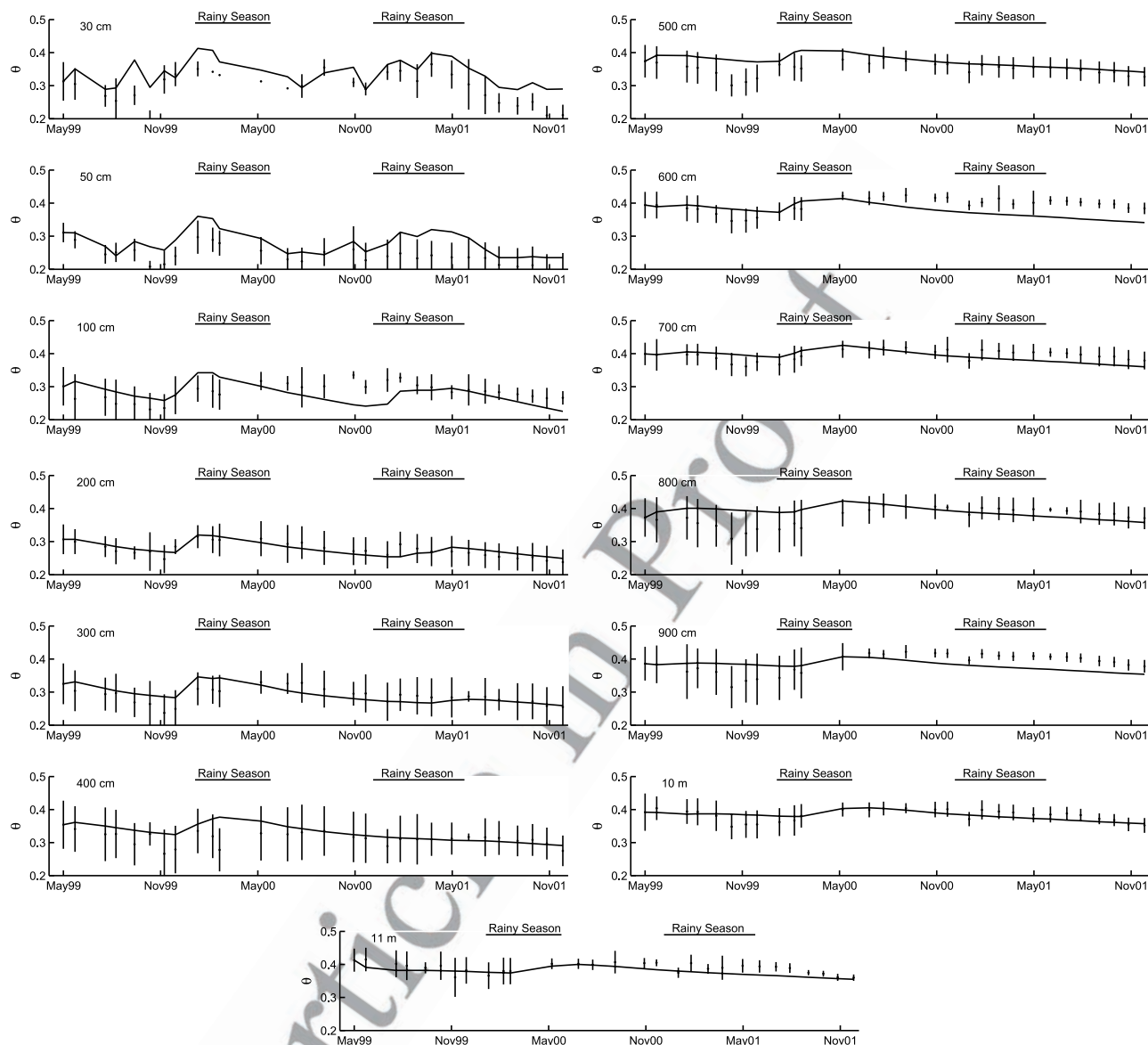


Figure 9. Monthly measured (dots) versus predicted (lines) volumetric water contents (θ) in the treatment plot, Tapajós National Forest, Brazil. Measured θ are averages of six TDR sensors per depth. Also shown are vertical bars representing measurement standard deviations, where available.

605 root growth at depth has been hypothesized [Nepstad *et al.*,
606 2002].

607 [50] Finally, recent work at this same site has demon-
608 strated a potential for hydraulic redistribution of water
609 through roots [Oliveira *et al.*, 2005]. Hydraulic redistribu-
610 tion can move water passively through roots either upward
611 or downward whenever a gradient in soil water potential
612 exists among soil layers which is stronger than the overall
613 gradient between soil and atmosphere. Hydraulic redistribu-
614 tion has been well documented in drier ecosystem but
615 only with this work has it been demonstrated in moist
616 tropical forest ecosystem. In fact, there was increased
617 evidence for downward hydraulic redistribution in the dry-
618 down plot of this study relative to the control [Oliveira
619 *et al.*, 2005]. Unfortunately, estimating the mass of water that
620 may move through these hydraulic processes is difficult.
621 The estimate for this site suggests as much as 10 percent of

rainfall inputs may be transported to deeper soils through this
622 process [Lee *et al.*, 2005]. 623

5. Hydrologic Budgets 625

[51] We compared the simulated hydrologic budgets for
626 both plots to further elucidate the mechanisms driving the
627 soil draw down observed in the treatment plot. Over the
628 960-day simulation period, there was an average of 5.3 mm
629 d^{-1} rainfall, 4.6 mm d^{-1} throughfall, and 0.63 mm d^{-1}
630 interception. On an annual basis, the 1925 mm of rainfall is
631 near the average of 2000 mm reported by Nepstad *et al.*
632 [2002] for this site. This 2-year average belies the fact that
633 in 2000 the rainfall was about 24 percent above normal
634 (2469 mm) and in 2001 rainfall was 10 percent below
635 normal (1798 mm). 636

[52] We estimated an average of 12 percent interception
637 of gross rainfall on the basis of data for our site. This value
638

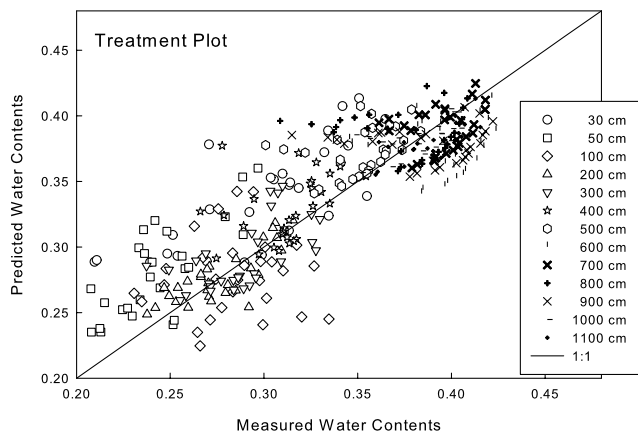


Figure 10. Scatterplot of measured and predicted volumetric water contents (θ) in the treatment plot, Tapajós National Forest, Brazil. The comparison is for 13 depths and 29 dates between May 1999 and December 2001 on which water content (θ) was measured at the field site.

639 is less than the 20 percent interception that *Nepstad et al.*
640 [2002] reported for the site during the 2000 rainy season. In
641 two other terra firme forest sites near Marabá and Ji-Paraná
642 in Brazil, *Ubarana* [1996] reported 13–14 percent inter-
643 ception, while in the Columbian Amazon, *Marin et al.*
644 [2000] report an interception of 13–18 percent.

646 5.1. Evapotranspiration

[53] In the control plot simulation the average evapora-
648 tion of 0.63 mm d^{-1} intercepted rainfall plus the average
649 transpiration of 3.07 mm d^{-1} plant uptake yielded an actual
650 evapotranspiration (AET) rate of 3.7 mm d^{-1} . Water bal-
651 ance studies have estimated AET rates of 4.15 mm d^{-1} for
652 an eastern Amazonian forest [*Jipp et al.*, 1998], 4.1 mm d^{-1}
653 for the central Amazon [*Leopoldo et al.*, 1995], and 3.59
654 and 3.65 mm d^{-1} for 2 years of field eddy correlation
655 measurements near Manaus [*Shuttleworth*, 1988; *da Rocha*
656 *et al.*, 1996]. Two recent eddy flux tower studies in close
657 proximity to our site within the Tapajós National Forest
658 measured AET at 3.45 mm d^{-1} for July 2000 to 2001 [*da*
659 *Rocha et al.*, 2004] or 3.1 mm d^{-1} for January 2002 to 2004
660 [*Hutyra et al.*, 2005]. The average control plot AET rate
661 also equals the value *Klinge et al.* [2001] simulated for an
662 eastern Amazonian forest from a model using the Penman
663 equation for PET and a matric head-dependent reduction
664 function.

[54] PET is typically higher in the July to December
666 dry season (5.0 mm d^{-1}) compared to the wet season
667 (4.1 mm d^{-1}) because of a higher vapor pressure gradient
668 between air and leaf surfaces. The model predicts that
669 AET is equal to PET for most of the year, except during
670 the dry season when soil moisture becomes limiting
671 (Figure 11). On average, AET was 80 percent of PET,
672 which is calculated to be 4.6 mm d^{-1} using the modified
673 Thornthwaite model.

[55] In the treatment plot simulation, AET declined by
675 0.125 mm d^{-1} . Considering the exclusion of throughfall by
676 the panels, only 2.85 mm d^{-1} water reached the soil in the
677 treatment plot, as opposed to 4.64 mm d^{-1} in the control
678 plot. Although less water is returned to the atmosphere in
679 the treatment plot simulation, AET is 25 percent higher than

the inputs that arrived at the soil surface. While evapotrans- 680
piration may exceed inputs for brief periods of time, the 681
water storage in the soil would become depleted if this were 682
to continue. 683

[56] Except for the top two layers, where uptake is 684
restricted during the dry season, the fraction of actual uptake 685
coming from each layer in the control plot strongly follows 686
the assumed root distribution. The same is true for the 687
treatment plot, although the uptake from the top two layers 688
is more restricted. The layers at 1 m and below became 689
slightly more important contributors to uptake as the exclu- 690
sion treatment continued. This interpretation excludes hy- 691
draulic redistribution, which indicates that water might be 692
redistributed from lower layers to upper layers allowing 693
plant uptake for evapotranspiration to continue from upper 694
layers [*Oliveira et al.*, 2005]. 695

5.2. Water Movement and Storage

[57] K_s varies from $3.2 \times 10^{-5} \text{ m s}^{-1}$ in the surface layer 698
to $8.2 \times 10^{-7} \text{ m s}^{-1}$ in the deepest layer (Figure 2). 699
Observed K_s values are large for clay-rich soils [*Hillel*, 700
1998], but are within the 2×10^{-7} to $6.4 \times 10^{-5} \text{ m s}^{-1}$ 701
range measured by researchers at another terra firme forest 702
site in Paragominas with similar, deeply weathered Oxisols 703
[*Moraes et al.*, 2006]. In fact, the range of variation, even 704
for a given depth, is not atypical for K_s measurements, 705
which can cover many orders of magnitude [*Rasmussen et* 706
al., 1993]. 707

[58] Not surprisingly, unsaturated hydraulic conductivity 708
($K(\theta)$) values are markedly reduced from the maximum 709
rates achieved at saturation. The simulated $K(\theta)$ for the 710
control plot are on the order of 10^{-7} m s^{-1} at the surface to 711
 10^{-9} m s^{-1} at other depths, while in the treatment plot the 712
simulated $K(\theta)$ are on the order of 10^{-8} m s^{-1} at the surface 713
to 10^{-9} m s^{-1} at other depths. 714

[59] The lower rates in the treatment plot mean that less 715
water drains past each layer than in the control, where water 716
fluxes are three to four times greater (Table 3). Before the 717
treatment was applied, similar amounts of water drained 718
through the profiles in both plots. After the panels were first 719
installed in early February 2000, the average control plot 720
fluxes went up because of the arrival of the rainy season. 721
However, in the treatment plot, the average fluxes decreased 722
at that time even with the increased rainfall. 723

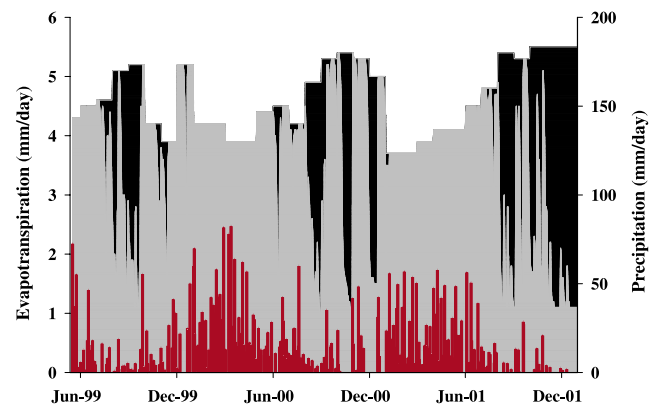


Figure 11. Potential evapotranspiration (PET) and simulated actual evapotranspiration (AET) for the Tapajós National Forest, Brazil. The dark areas represent periods of water deficit when AET is less than PET.

t3.1 **Table 3.** Simulated Fluxes of Water in the Control Plot and Throughfall Exclusion Treatment Plot, Tapajós National Forest, Brazil^a

		Control						Treatment					
		Pre	W1	D1	W2	D2	Total	Pre	W1	D1	W2	D2	Total
t3.4	Rainfall	1.21	1.50	0.59	1.55	0.25	5.10	1.21	1.50	0.59	1.55	0.25	5.10
t3.5	Interception	0.14	0.18	0.07	0.19	0.03	0.61	0.14	0.18	0.07	0.19	0.03	0.61
t3.6	Exclusion	0.00	0.00	0.00	0.00	0.00	0.00	0.00	0.80	0.12	0.81	0.00	1.73
t3.7	Throughfall	1.07	1.32	0.52	1.36	0.22	4.49	1.06	0.52	0.40	0.55	0.22	2.75
t3.8	Actual ET	0.98	0.63	0.75	0.72	0.51	3.59	0.98	0.61	0.65	0.72	0.47	3.43
t3.9	Flux												
t3.10	0.40 m depth	0.51	1.08	0.18	1.02	0.03	2.82	0.51	0.27	0.08	0.16	0.02	1.04
t3.11	0.75 m depth	0.39	0.93	0.12	0.85	0.01	2.31	0.39	0.23	0.02	0.11	0.00	0.75
t3.12	1.50 m depth	0.34	0.93	0.13	0.82	0.03	2.24	0.34	0.25	0.00	0.06	0.00	0.65
t3.13	2.50 m depth	0.35	0.93	0.15	0.76	0.05	2.23	0.35	0.27	0.01	0.02	0.00	0.65
t3.14	3.50 m depth	0.34	0.93	0.18	0.69	0.09	2.22	0.34	0.30	0.02	0.00	0.00	0.66
t3.15	4.50 m depth	0.32	0.92	0.20	0.63	0.12	2.19	0.32	0.31	0.04	0.00	0.00	0.67
t3.16	5.50 m depth	0.32	0.90	0.22	0.58	0.15	2.16	0.32	0.30	0.05	0.01	0.00	0.68
t3.17	6.50 m depth	0.34	0.85	0.24	0.53	0.19	2.14	0.34	0.27	0.07	0.02	0.00	0.70
t3.18	7.50 m depth	0.36	0.80	0.25	0.48	0.21	2.11	0.36	0.24	0.09	0.02	0.00	0.71
t3.19	8.50 m depth	0.36	0.76	0.28	0.44	0.24	2.07	0.36	0.21	0.11	0.03	0.01	0.72
t3.20	9.50 m depth	0.37	0.71	0.29	0.40	0.27	2.05	0.37	0.18	0.12	0.04	0.01	0.74
t3.21	10.50 m depth	0.38	0.67	0.31	0.36	0.30	2.02	0.38	0.16	0.14	0.05	0.02	0.75
t3.22	11.50 m depth	0.40	0.63	0.34	0.33	0.33	2.03	0.40	0.14	0.16	0.06	0.03	0.80
t3.23	Δ Soil Storage	-0.43	0.45	-0.45	0.50	-0.60	-0.53	-0.21	-0.04	-0.33	-0.05	-0.26	-0.89

t3.24 ^aThe pretreatment period (Pre) is May 1999 to January 2000; the first wet season (W1) is February to June 2000; the first dry season (D1) is July to December 2000; the second wet season (W2) is January to June 2001; and the second dry season (D2) is July to December 2001. All units are in meters.

724 [60] The fraction of water lost to deep drainage is smaller
 725 under the treatment. In the control plot, about 45 percent of
 726 water input to the soil is drained past 11.5 m, compared to
 727 17 percent in the treatment plot. The negative change in water
 728 storage in the control plot is an artifact of the 960-day time span
 729 for which the simulated fluxes of Table 3 are reported. This
 730 period covers both pretreatment and posttreatment periods and
 731 includes three dry seasons but only two wet seasons.

732 [61] The measured water content in the control plot over
 733 the entire simulation period clearly demonstrates that soil
 734 moisture was recharged during the 2001 rainy season
 735 (Figure 12). The measured water contents in the control
 736 plot also show that the soils at depth are wetter than near the
 737 surface. During the dry season, water is withdrawn from the
 738 entire profile, especially in the upper profile where there is a
 739 higher concentration of roots. By the middle of the rainy
 740 season, the surface soils rewet and the water storage below
 741 4 m recharges.

742 [62] The soils in the treatment plot were drier than the
 743 soils in the control plot even before the exclusion panels
 744 were first installed in February 2000 (Figure 12). Because
 745 the dry season preceding the first treatment period and the
 746 treatment period itself were wetter than average, the panels
 747 did not divert sufficient water to invoke drought stress in the
 748 vegetation within the treatment plot [Nepstad *et al.*, 2002].
 749 However, during the second treatment period, the soil near
 750 the surface dried more extensively and recharge at depth
 751 was not complete. The predicted water contents show
 752 similar patterns with depth, the most notable difference
 753 being that the current model predicts that the soil below
 754 5 m in the treatment plot dries out more than measured
 755 during the second treatment year.

757 6. Conclusions

758 [63] A soil water model using Darcy's law and Richard's
 759 equation is presented for the purpose of evaluating unsatu-

760 rated water fluxes and storage in a moist tropical forest soil.
 761 Model predictions are compared with soil water content
 762 estimates.

763 [64] The one-dimensional model used in this study pre-
 764 dicted soil volumetric water content within 3 percent of water
 765 content measures obtained using TDR probes in six 11-m-
 766 deep soil shafts for the first 960 days of a throughfall
 767 reduction experiment under a moist tropical forest. This
 768 accuracy of prediction is quite impressive and indicates that
 769 physical processes of soil water movement in the ecosystem
 770 are captured by the model even despite the relatively coarse
 771 vertical and temporal scale of modeling. Landscapes with
 772 more complex terrain may require models with additional
 773 dimensions, but one-dimensional, vertical flow seems ap-
 774 propriate for this well-drained plateau site, a common
 775 feature in the Amazon basin.

776 [65] The model is sensitive to the van Genuchten param-
 777 eters, θ_s , θ_r , and n , but less sensitive to K_s and α . These
 778 parameters are used to translate water content to head and to
 779 determine the unsaturated water flow function. Theoretically,
 780 the water retention properties these parameters describe are
 781 physical properties of the soil that can be quantified, although
 782 in our model we needed to calibrate these parameters to
 783 reproduce the observed soil moisture data.

784 [66] During the first year of throughfall exclusion, the
 785 measured water contents demonstrate, and the model pre-
 786 dicted, mild soil water depletion near the surface. Persistence
 787 of the drought into a second year leads to more extensive
 788 drying of the surface soils and prevented complete recharge
 789 of water stored deeper in the soil. The model predicts that
 790 evapotranspiration declined during this period, and that
 791 water drainage was diminished. More importantly, however,
 792 our model shows that decreases in evapotranspiration were
 793 marginal while decreases in water flux were substantial.

794 [67] Clearly, soil water stores were being depleted by a
 795 reduction in soil moisture inputs. Over prolonged periods of
 796 drought this imbalance between water inputs and evapo-

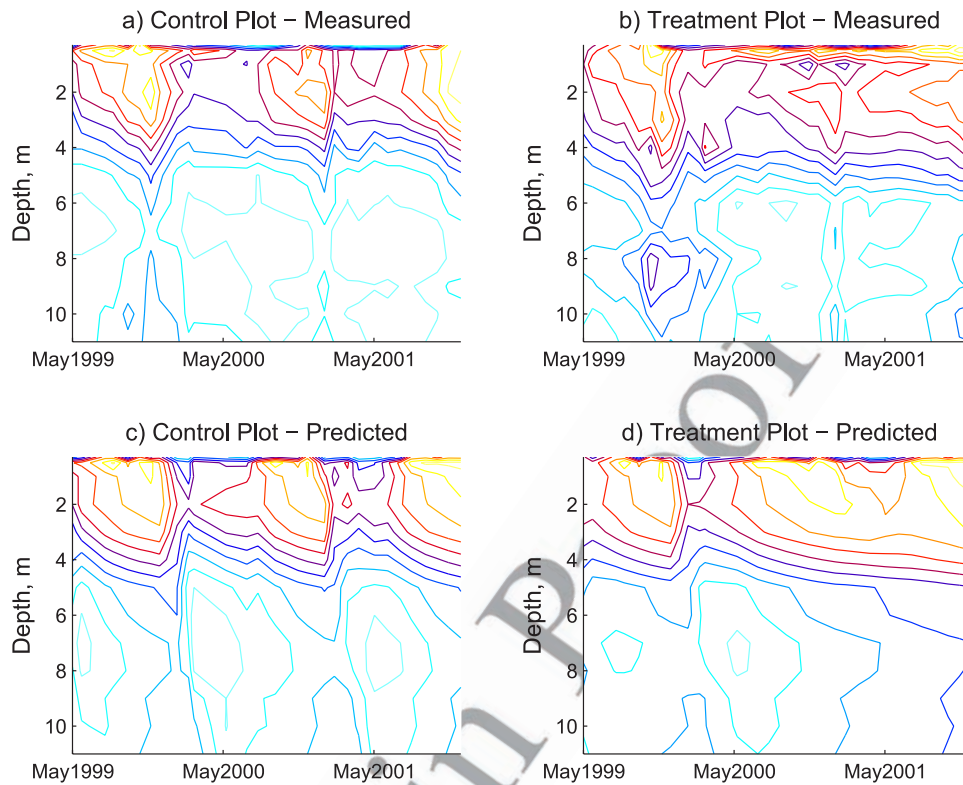


Figure 12. Measured water contents ($\text{m}^3 \text{m}^{-3}$) in the (a) control and (b) treatment plots and simulated water contents in the (c) control and (d) treatment plots, Tapajós National Forest, Brazil. Each depth is an average of six TDR sensors. Range of water contents is from 0.18 to 0.46 in increments of 0.02. Drier soils are marked in red and wetter soils in blue. Throughfall reduction in the treatment plot commenced at the start of the 2000 rainy season.

797 transpiration are unsustainable once soil moisture reserves
 798 are exhausted. In fact, it is exactly such an increase in
 799 drought severity that has been predicted in response to
 800 global climate change that could exceed the limit of drought
 801 tolerance of these moist tropical forests, which the contin-
 802 uation of this experiment is designed to test.

803 [68] **Acknowledgments.** We wish to thank David Radcliffe, Miguel
 804 Cabrera, John Dowd, A. Marysol Schuler, David Redman, and Paul
 805 Lefebvre, as well as the researchers at the Woods Hole Research Center
 806 and the Instituto de Pesquisa Ambiental da Amazônia for their various
 807 contributions to this project. Field aspects of this research were funded by
 808 NSF grant DEB 9707566. The UGA Graduate School provided salary
 809 support for the lead author during model development. We also thank the
 810 Instituto Brasileiro do Meio Ambiente e dos Recursos Naturais Renováveis
 811 for logistical support on the Tapajós National Forest.

812 References

813 Baker, J. M., and R. J. Lascano (1989), The spatial sensitivity of time
 814 domain reflectometry, *Soil Sci.*, 147(5), 378–383.
 815 da Rocha, H. R., P. J. Sellers, G. J. Collatz, I. Wright, and J. Grace (1996),
 816 Calibration and use of the *SiB2* model to estimate water vapour and
 817 carbon exchange at the ABRACOS forest sites, in *Amazonian Deforestation*
 818 *and Climate*, edited by J. H. C. Gash et al., pp. 459–471, John
 819 Wiley, New York.
 820 da Rocha, H. R., M. L. Goulden, S. D. Miller, M. C. Menton, L. D. V. O.
 821 Pinto, H. C. de Freitas, and A. M. e Silva Figueira (2004), Seasonality of
 822 water and heat fluxes over a tropical forest in eastern Amazonia, *Ecol.*
 823 *Appl.*, 14, S22–S32.
 824 Davidson, E. A., and S. E. Trumbore (1995), Gas diffusivity and production
 825 of CO_2 in deep soils of the eastern Amazon, *Tellus, Ser. B*, 47, 550–565.
 826 de Amorim, M. C., L. Rossato, and J. Tomasella (1999), Determinação da
 827 evapotranspiração potencial do Brasil aplicado o modelo de Thornthwaite

a um sistema de informação geografica, *Rev. Bras. Recur. Hidricos*, 4(3), 828
 83–90. 829
 Feddes, R. A., P. J. Kowalik, and H. Zaradny (1978), *Simulation of Field* 830
Water Use and Crop Yield, 189 pp., John Wiley, New York. 831
 Feddes, R. A., et al. (2001), Modeling root water uptake in hydrological and 832
 climate models, *Bull. Am. Meteorol. Soc.*, 82(12), 2797–2809. 833
 Hillel, D. (1998), *Environmental Soil Physics*, 771 pp., Academic, San 834
 Diego, Calif. 835
 Hodnett, M. G., and J. Tomasella (2002), Marked differences between van 836
 Genuchten soil water-retention parameters for temperate and tropical 837
 soils: New water-retention pedo-transfer functions developed for tropical 838
 soils, *Geoderma*, 108, 155–180. 839
 Hutya, L. R., J. W. Munger, C. A. Nobre, S. R. Saleska, S. A. Vieira, and 840
 S. C. Wofsy (2005), Climatic variability and vegetation vulnerability in 841
 Amazônia, *Geophys. Res. Lett.*, 32, L24712, doi:10.1029/
 2005GL024981. 842
 Jipp, P. H., D. C. Nepstad, K. Cassel, and C. R. de Carvalho (1998), Deep 843
 soil moisture storage and transpiration in forests and pastures of season- 844
 ally-dry Amazonia, *Clim. Change*, 39, 395–413. 845
 Jordan, C. F., and J. Heuvelop (1981), The water budget of an Amazonian 846
 rain forest, *Acta Amazonica*, 11, 87–92. 847
 Klinge, R., J. Schmidt, and H. Folster (2001), Simulation of water drainage 848
 of a rain forest and forest conversion plots using a soil water model, 849
J. Hydrol., 246, 82–95. 850
 Klute, A., and C. Dirksen (1986), Hydraulic conductivity and diffusivity: 851
 Laboratory methods, in *Methods of Soil Analysis*, part 1, *Physical and* 852
Mineralogical Methods, *Soil Sci. Soc. Am. Agron. Monogr.*, vol. 9, edited 853
 by A. Klute, pp. 687–734, Soil Sci. Soc. of Am., Madison, Wis. 854
 Knight, J. H. (1992), Sensitivity of time domain reflectometry measure- 855
 ments to lateral variations in soil water content, *Water Resour. Res.*, 856
 28(9), 2345–2352. 857
 Knight, J. H., I. White, and S. J. Zegelin (1994), Sampling volume of TDR 858
 probes used for water content monitoring, in *Proceedings From* 859
the Symposium on TDR in Environmental, Infrastructure, and Mining 860
Applications, Northwestern University, Evanston, IL, Sept. 7–9, 1994, 861
 862

- 863 *Spec. Publ. SP 19-94*, pp. 93–104, Bur. of Mines, U.S. Dep. of the Inter.,
864 Washington, D. C.
- 865 Lee, D. H., and L. M. Abriola (1999), Use of Richards' equation in land
866 surface parameterizations, *J. Geophys. Res.*, 104(D22), 27,519–
867 27,526.
- 868 Lee, J., R. S. Oliveira, T. E. Dawson, and I. Fung (2005), Root functioning
869 modifies seasonal climate, *Proc. Natl. Acad. Sci. U.S.A.*, 102(49),
870 17,576–17,581.
- 871 Leopoldo, P. R., W. K. Franken, and N. Augusto Villa Nova (1995), Real
872 evapotranspiration and transpiration through a tropical rain forest in cen-
873 tral Amazonia as estimated by the water balance method, *For. Ecol.*
874 *Manage.*, 73, 185–195.
- 875 Marin, C. T., W. Bouten, and J. Sevink (2000), Gross rainfall and its
876 partitioning into throughfall, stemflow and evaporation of intercepted
877 water in four forest ecosystems in western Amazonia, *J. Hydrol.*, 237,
878 400–457.
- 879 Monteith, J. L. (1965), Evaporation and the environment, in *The Movement*
880 *of Water in Living Organisms, XIXth Symposium of the Society for Ex-*
881 *perimental Biology, Swansea*, edited by G. E. Fogg, pp. 205–234, Cam-
882 bridge Univ. Press, New York.
- 883 Moraes, J. M., A. E. Schuler, T. Dunne, R. de O. Figueiredo, and R. L.
884 Victoria (2006), Water storage and runoff processes in plinthic soils
885 under forest and pasture in eastern Amazonia, *Hydrol. Processes*, 20,
886 2509–2526.
- 887 Mualem, Y. (1976), A new model for predicting the hydraulic conductivity
888 of unsaturated porous media, *Water Resour. Res.*, 12(3), 513–522.
- 889 Muller, C. (1999), *Modelling Soil-Biosphere Interactions*, 354 pp., CABI,
890 Cambridge, U. K.
- 891 Nepstad, D. C., et al. (2002), The effects of partial throughfall exclusion on
892 canopy processes, aboveground production, and biogeochemistry of an
893 Amazon forest, *J. Geophys. Res.*, 107(D20), 8085, doi:10.1029/
894 2001JD000360.
- 895 Nepstad, D. C., P. Lefebvre, U. L. Lopes, J. Tomasella, P. Schlesinger,
896 L. Solorzano, P. Moutinho, D. Ray, and J. G. Benito (2004), Amazon
897 drought and its implications for forest flammability and tree growth: A
898 basin-wide analysis, *Global Change Biol.*, 10, 704–717, doi:10.1111/
899 j.1529-817.2003.00772.x.
- 900 Oliveira, R. S., T. E. Dawson, S. S. O. Burgess, and D. C. Nepstad (2005),
901 Hydraulic redistribution in three Amazonian trees, *Oecologia*, 145, 354–
902 363, doi:10.1007/s00442-005-0108-2.
- 903 Rasmussen, T. C., D. D. Evans, P. J. Sheets, and J. H. Blanford (1993),
904 Permeability of Apache Leap Tuff: Borehole and core measurements
905 using water and air, *Water Resour. Res.*, 29(7), 1997–2006.
- 906 Rasmussen, T. C., R. H. Baldwin, J. F. Dowd, and A. G. Williams (2000),
907 Tracer vs. pressure wave velocities through unsaturated saprolite, *Soil*
908 *Sci. Soc. Am. J.*, 64(1), 75–85.
- Richter, D. D., and L. I. Babbar (1991), Soil diversity in the tropics, *Adv.*
Ecol. Res., 21, 315–389. 909
- Schlesinger, W. H. (1997), *Biogeochemistry: An Analysis of Global*
Change, 588 pp., Academic, New York. 910
- Shuttleworth, W. J. (1988), Evaporation from Amazonian rain forest, *Proc.*
R. Soc. London, Ser. B, 233(1272), 321–346. 911
- Šimůnek, J., M. T. van Genuchten, and M. Šejna (2005), The HYDRUS-1D
software package for simulating the movement of water, heat, and multiple
solutes in variably saturated media, version 3.0, *HYDRUS Software Ser.*,
vol. 1, Dep. of Environ. Sci., Univ. of Calif., Riverside, Calif. 912
- Soil Moisture Equipment Corporation, (1986), Guelph permeameter
2800K1 operating instructions, Santa Barbara, Calif. 913
- Sternberg, L. D. S. L., M. Moreira, and D. C. Nepstad (2002), Uptake of
water by lateral roots of small trees in an Amazonian tropical forest,
Plant Soil, 238, 151–158. 914
- Thornthwaite, C. W., and J. R. Mather (1957), *Instructions and Tables for*
Computing Potential Evapotranspiration and the Water Balance, 311 pp.,
Drexel Inst. of Technol., Lab. of Climatol., Centerton, N. J. 915
- Topp, G. C., J. L. Davis, and A. P. Annan (1980), Electromagnetic deter-
mination of soil water content: Measurements in coaxial transmission
lines, *Water Resour. Res.*, 16(3), 574–582. 916
- Ubarana, V. N. (1996), Observations and modelling of rainfall interception
at two experimental sites in Amazonia, in *Amazonian Deforestation and*
Climate, edited by J. H. C. Gash et al., pp. 151–162, John Wiley, New
York. 917
- van Genuchten, M. T. (1980), A closed-form equation for predicting the
hydraulic conductivity of unsaturated soils, *Soil Sci. Soc. Am. J.*, 44,
892–898. 918
- Wraith, J. M., S. D. Comfort, B. L. Woodbury, and W. P. Inskeep (1993),
A simplified waveform analysis approach for monitoring solute trans-
port using time-domain reflectometry, *Soil Sci. Soc. Am. J.*, 57, 637–
642. 919
- Zegelin, S. J., I. White, and D. R. Jenkins (1989), Improved field probes for
soil water content and electrical conductivity measurement using time
domain reflectometry, *Water Resour. Res.*, 25(11), 2367–2376. 920
-
- E. L. Belk, U.S. Environmental Protection Agency, 61 Forsyth Street, 944
Atlanta, GA 30303-8960, USA. 945
- E. J. M. Carvalho, Embrapa Amazônia Oriental, Caixa Postal 48, CEP 947
66095-100, Belém, Pará, Brazil. 948
- E. A. Davidson and D. C. Nepstad, Woods Hole Research Center, 949
P.O. Box 296, Woods Hole, MA 02345, USA. 950
- D. Markewitz and T. C. Rasmussen, Warnell School of Forestry and 951
Natural Resources, University of Georgia, Athens, GA 30602-2152, USA. 952
(dmarke@warnell.uga.edu) 953